Acta Crystallographica Section D
Biological Crystallography
ISSN 0907-4449

Effect of pH on the structure of rhizopuspepsin

B. V. L. S. Prasad and K. Suguna*

Molecular Biophysics Unit, Indian Institute of Science, Bangalore 560 012, India

Correspondence e-mail: suguna@mbu.iisc.ernet.in

Received 27 February 2003
Accepted 21 July 2003

PDB References: rhizopuspepsin, pH 4.6, 1uh7, r1uh7sf; pH 7.0, 1uh9, r1uh9sf; pH 8.0, 1uh8, r1uh8sf.

The crystal structure of rhizopuspepsin has been determined at three different pH values (4.6, 7.0 and 8.0) and compared with the previously reported structure at pH 6.0. A pH-sensitive region in the protein has been identified where certain structural changes take place at pH 8.0. An increase in the mobility of loops, weakening of hydrogen bonding and ionic interactions and a change in the water structure have been observed in this region. The loop between the first and the second β-strands of the N-terminus shows increased mobility at high pH. This loop is known to be highly flexible in aspartic proteinases, aiding in relocating the N-terminal β-strand segment in pH-related structural transformations. The observed changes in rhizopuspepsin indicate the triggering of a possible denatured state by high pH. The conformation of the active aspartates and the geometry of the catalytic site exhibit remarkable rigidity in this pH range.

1. Introduction

Aspartic proteinases found in a large number of organisms have been shown to perform a variety of biological functions (Davies, 1990). They have been identified as potential targets for developing drugs against fatal diseases such as AIDS owing to their involvement in the life cycle of pathogenic organisms. They catalyze peptide-bond hydrolysis with the involvement of two active aspartates. The members of the pepsin family have a bilobal structure, with the active-site cleft located between the lobes. The catalytic aspartates (Asp32 and Asp215; pepsin numbering) are contributed from each lobe. These residues are situated within the motif D-S/T-G, known as the signature sequence of the aspartic proteinase family. In spite of having similar tertiary structure and active-site geometry, aspartic proteinases differ significantly in substrate specificity and pH optimum. It is well known that each one of the aspartic proteinases has a characteristic pH optimum that can vary from pH 2 for mammalian pepsins to a value of more than 7 for renin.

Aspartic proteinases exhibit pH-dependent activity. The digestion of food material, the processing of proteins, protein turnover and activation of zymogens are a few examples which are directly influenced by pH. The pH-rate profiles of these enzymes suggest that during catalysis the active aspartates exist in the mono-protonated state. Recent neutron Laue diffraction studies (Coates *et al.*, 2001) have confirmed that one of the active aspartates is protonated and the other is negatively charged, as proposed based on X-ray crystallographic studies (Davies, 1990), supporting the general acid–base catalysis mechanism. It was reported that in solution the N-terminal β-strand segment of porcine pepsin plays a role in the alkaline inactivation/denaturation of the enzyme (Lin *et*

Table 1
Crystallization conditions for various pH forms of rhizopuspepsin.

pH	Condition
4.6	Drop: 2 µl of 14 mg ml^{-1} protein concentration and 2 µl of reservoir solution. Reservoir solution: 500 ml 30% PEG 4K, 0.1 *M* sodium acetate, 0.2 *M* ammonium acetate.
6.0†	Sitting-drop method: 14 mg ml^{-1} protein solution containing 20 m*M* calcium acetate and 50 m*M* cacodylate buffer.
7.0	Drop: 2 µl of 14 mg ml^{-1} protein concentration and 2 µl of reservoir solution. Reservoir solution: 500 ml of 0.8 *M* K,Na tartrate, 0.1 *M* Na HEPES.
8.0	Sitting-drop method: 14 mg ml^{-1} protein solution containing 20 m*M* calcium acetate and 50 m*M* cacodylate buffer.

† The reference pH form.

Table 2
Statistics of X-ray intensity data.

Values in parentheses are for the last shell.

	pH		
	4.6	7.0	8.0
Unit-cell parameters (Å)			
a	60.48	60.19	60.37
b	60.52	60.79	60.58
c	106.87	106.99	107.36
Unit-cell volume (Å^3)	391190	392117	392667
Completeness (%)	94.5 (90.7)	99.8 (99.8)	97.1 (97.0)
Resolution limit (Å)	2.1	2.0	2.3
No. of reflections	134320	182501	93785
Unique reflections	22317	27185	17618
$R_{\rm merge}$ (%)	9.3 (30)	7.8 (28.3)	8.9 (32)
Mosaicity	0.35	0.28	0.18

al., 1993; Tanaka & Yada, 2001). The same segment, which is located in the active-site cleft in its proenzyme as well as in prophytepsin and proplasmepsin, undergoes a conformational change following a large movement to become a part of the central six-stranded β-sheet at the back of the protein upon activation by acidification (Bernstein & James, 1999).

There have been a number of crystallographic studies aimed at understanding the structural basis of pH-induced changes in proteins. Some proteins do not undergo any significant changes in their structures with change in pH, as in the case of lysozyme studied at three different pH values (4.6, 6.5 and 9.5; Biswal *et al.*, 2000). A recent study of the crystal structure of ribonuclease A at five different pH values at atomic resolution provided better insight into the catalytic role played by Lys41 (Berisio *et al.*, 2002). Some interesting results have been noticed in staphylococcal enterotoxin C2 (Kumaran *et al.*, 2001) and plastocyanin (Guss *et al.*, 1986), where the coordination distances of the metal ions from the protein atoms increase gradually with decreasing pH. Other pH-induced changes in crystal structures include rotation of the side chains in cubic insulin (Gursky *et al.*, 1992), γ-chymotrypsin (Dixon *et al.*, 1991) and myoglobin (Yang & Phillips, 1996), peptide-bond flipping in azurin (Nar *et al.*, 1991) and changes observed in the tertiary structure of α-chymotrypsin (Vendlen & Tulinsky, 1973; Mavridis *et al.*, 1974) and in the catalytic loop of avian sarcoma virus integrase (Lubkowski *et al.*, 1999).

Some protein structures exhibit significant pH-dependent structural changes. The most dramatic change was reported in the surface glycoprotein of influenza virus. The haemagglutinin exists in a retracted state under normal conditions, as the peptide that binds to the sialylated cell-surface receptor is buried from the distal tip of the protein and is therefore incapable of binding to the cell membrane. However, at low pH a major conformational change occurs as the fusion peptide moves at least 100 Å and is delivered *via* a spring-loaded mechanism to the distal tip, where it is available to bind to the cell membrane (Carr & Kim, 1993; Bullough *et al.*, 1994). The crystal structure of cathepsin D, an aspartic proteinase involved in protein turnover, has been solved in the active form (pH 5.1) and also at a higher pH (pH 7.5). At higher pH, the first strand of the six-stranded inter-domain β-sheet moves a distance of 30 Å into the active site, rotating by approximately 180° and blocking the active aspartates (Lee *et al.*, 1998). Moreover, the strand itself changes into a random coil. This analysis and comparison of the structures of proenzymes with their active forms (Bernstein & James, 1999) indicate that this N-terminal segment possesses inherent flexibility and the ability to adopt different conformations. These observations have important implications in understanding the structural basis of the pH-dependent regulation of protein activity and pH-dependent modulation of substrate specificity.

In view of the importance of the phenomenon and owing to the fact that pH-induced structural analysis exists for only one of the aspartic proteinases as mentioned in the previous paragraph, we are interested in investigating the effect of pH on the protein and solvent structure of aspartic proteinases by means of X-ray crystallography. To probe whether the structure undergoes any changes on variation of the pH which in turn may influence its activity, we have determined the crystal structure of rhizopuspepsin, a fungal aspartic proteinase, in three different forms at pH values of 4.6, 7.0 and 8.0. A detailed comparison of the different pH forms including the previously reported crystal form at pH 6.0 has been carried out. We discuss the insights obtained from this analysis on the effect of pH on the structure and its implications for the function of the enzyme.

2. Materials and methods

Rhizopuspepsin, obtained as a gift from Dr D. R. Davies of the National Institutes of Health, USA, was originally provided by Robert Delaney of the University of Oklahoma and was previously crystallized at pH 6.0 using the sitting-drop method. The structure was determined at 1.8 Å resolution (Suguna *et al.*, 1987). It crystallized in space group $P2_12_12_1$, with unit-cell parameters $a = 60.31$, $b = 60.60$, $c = 106.97$ Å. We have now obtained crystals of rhizopuspepsin at pH 4.6, pH 7.0 and pH 8.0 by the hanging-drop method. For all the pH forms, large crystals of dimensions $0.8 \times 0.5 \times 0.3$ mm grew within a week at 277 and at 293 K. The crystallization conditions are given in Table 1.

Intensity data were collected at 293 K from crystals grown at pH 4.6, 7.0 and 8.0 on MAR300 imaging plate mounted on a

Rigaku RU-200 rotating-anode X-ray generator with an Osmic mirror for collimation. The crystal-to-detector distance was maintained at 120 mm in all experiments. Care was taken to ensure that the data-collection conditions were identical in all cases. All data sets were processed in an identical manner using *DENZO* and *SCALEPACK* (Otwinowski & Minor, 1997). Details of data collection and processing are given in Table 2.

The atomic coordinates of the pH 6.0 form of rhizopuspepsin (Suguna *et al.*, 1987; PDB code 2apr) were used as the starting model for the refinements. All four structures including 2apr (refined earlier using *PROLSQ*; Hendrickson & Konnert, 1981) were refined in an identical manner using the program *CNS* v.1.0 (Brünger *et al.*, 1998). The entire molecule was treated as a rigid body in the initial cycles of refinement. This was followed by *B*-factor group, positional and *B*-factor individual refinements, calculation of the electron-density maps and model building/checking using the program *O* (Jones *et al.*, 1991). In the subsequent stages of refinement and model building, peaks greater than 3σ in $F_o - F_c$ maps and 1σ in $2F_o - F_c$ maps were identified as water O atoms. In the later cycles, the cutoff values were reduced to 2.5σ and 0.8σ, respectively. Bulk-solvent correction and anisotropic scaling were used throughout the process. The final *R* factors were in the range 14–16% (Table 3). The stereochemical quality of the structures was validated using *PROCHECK* (Laskowski *et al.*, 1993). The solvent structure constituting the primary hydration shell or the first hydration shell (Prasad & Suguna, 2002) was identified for all four pH forms. The protein structures at pH 4.6, 7.0 and 8.0 along with the respective primary hydration waters were superposed on the pH 6.0 form, the reference structure for this analysis, using the program *ALIGN* (Cohen, 1997) using the C^{α} atoms, main-chain atoms, main-chain and C^{β} atoms and all atoms. The r.m.s.d. values are given in Table 3. The aligned coordinates were used to find the conserved or equivalent waters among all the pH forms. The hydrogen bonds (distance < 3.6 Å, angles N—H···Wat > 120° and C—O···Wat > 90°) were calculated for all the conserved waters. Water–water hydrogen bonds were assigned based on the distance cutoff only.

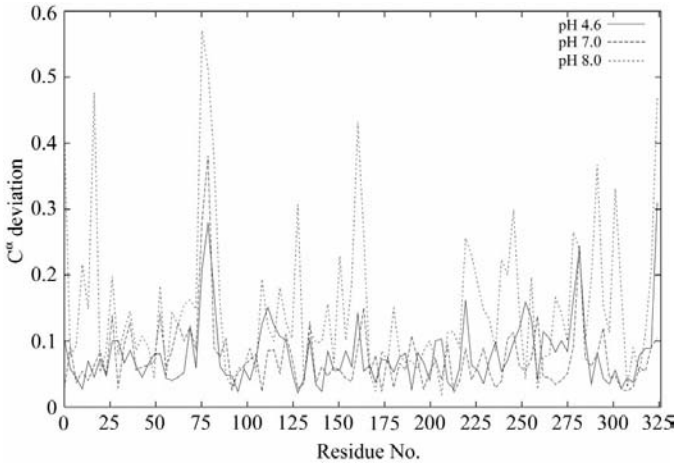

Figure 1
C^{α} deviations of different pH forms of rhizopuspepsin from the pH 6.0 form.

Table 3
Refinement statistics.

	pH			
	4.6	6.0†	7.0	8.0
R factor	0.147	0.156	0.157	0.158
R_{free} value	0.179	0.183	0.194	0.201
Average *B* factors (Å^2)				
Main chain	17.92	24.35	20.09	27.75
Side chain	19.92	26.95	22.47	30.06
Solvent	35.53	44.35	39.39	41.63
No. of protein atoms	2402	2402	2402	2402
No. of solvent molecules	336	365	386	296
No. of primary waters	326	336	343	273
No. of invariant waters	295	—	300	249
R.m.s. deviations from ideality				
Bond lengths (Å)	0.005	0.005	0.005	0.005
Bond angles (°)	1.3	1.3	1.3	1.3
Dihedral angles (°)	26.4	26.2	26.5	26.2
Improper angles (°)	0.75	0.74	0.74	0.75
Residues in core region of φ–ψ plot (%)	93.6	95.1	94.7	92.4
Residues in the additionally allowed region (%)	6.4	4.9	5.3	7.6
Overall r.m.s. deviation of C^{α} atoms (Å)	0.083	—	0.075	0.158

† The reference pH form reported earlier (PDB code 2apr) has been re-refined.

3. Results and discussion

The structures refined in the present study are those at pH 4.6, 7.0 and 8.0. Rhizopuspepsin could not be crystallized outside the pH 4.6–8.0 range. Although the crystallization conditions at pH 7.0 and pH 4.6 are different from the conditions that give crystals of the other two forms, the proteinase crystallized in the same orthorhombic space group $P2_12_12_1$. A plot of the deviations of the C^{α} atoms of the pH 4.6, 7.0 and 8.0 forms from the pH 6.0 form shown in Fig. 1 and the r.m.s.d. values given in Table 3 clearly indicate that compared with the pH 8.0 form, the other forms show much smaller deviations. In the final refined models, 92.4–95.1% of the residues lie in the most favoured regions of the Ramachandran plot (Ramachandran *et al.*, 1963). The percentage of residues in the additionally allowed regions is higher in the pH 8.0 form. No residues are found in the generously allowed or disallowed regions. The regions consisting of residues 9–20, 73–80, 154–165 and 289–295 show comparatively higher deviations, indicating an inherent flexibility of these loops. These deviations are more pronounced in the case of the pH 8.0 form (Fig. 1).

An important observation that has emerged from comparing various pH forms is that the geometry of the catalytic site and the conformation of the active aspartates Asp35 and Asp218 remain unchanged in the pH range 4.6–8.0. The hydrogen bonds between the aspartates and those between the catalytic water, Wat507, and the aspartates are also conserved. The side-chain torsion angles of most of the residues are unaffected by pH, except for a few charged and hydrophilic residues on the surface of the protein in which a small variation in the χ values (about 5–10°) has been observed.

3.1. *B* factors and stability

Individual *B* factors provide a good estimate of the flexibility of the protein; in particular, when the *B* factors of the same molecule in different environments are compared, one may obtain information about the effect of external factors on various regions of the protein. Hence, to further explore the structural changes between the various pH forms, the *B* factors of protein atoms and water molecules were carefully examined. A plot of the normalized *B* factors $[(B - \langle B\rangle)/\sigma(B)]$ of the C^{α} atoms in all the pH forms is shown in Fig. 2. The average *B* factors of the main-chain and the side-chain atoms and water molecules in the crystal structures presented here are listed in Table 3. The pH 8.0 form shows considerably higher *B* factors when compared with the others. It was shown in earlier studies that the 'flap' region formed by residues 72–83 and a variable loop region consisting of residues 290–295 of the C-terminal domain are highly flexible in all aspartic proteinases (Sali *et al.*, 1992). However, the recent crystal structure of cathepsin D at high pH (PDB code 1lyw; pH 7.5; Lee *et al.*, 1998) has shown that the β-hairpin turn, residues 8–15 (equivalent to residues 10–17 in rhizopuspepsin), is also a very flexible region with a tendency to change its conformation. The effect of pH on the *B* factors is clearly evident from Figs. 2 and 3. Residues with relatively higher *B* factors in the crystal structure at pH 8.0 are Asn13 (80.17 Å^2 for C^{α} and 91.23 Å^2 for OD1), Asp79 (72.80 Å^2 for C^{α} and 75.65 Å^2 for OD2), Lys162 (70.73 for C^{α} and 83.72 Å^2 for NZ) and Glu325 (66.45 Å^2 for C^{α} and 89.40 Å^2 for OE1). All these residues are located in loops which are in close proximity in the structure (Fig. 3). The flap region has the highest *B* factors in the form at pH 4.6, the pH at which rhizopuspepsin has maximum catalytic efficiency (Hofmann *et al.*, 1984). This observation suggests that it is important for the flap to be as flexible as possible for the substrate to enter the binding cleft at the optimum pH to accomplish catalysis.

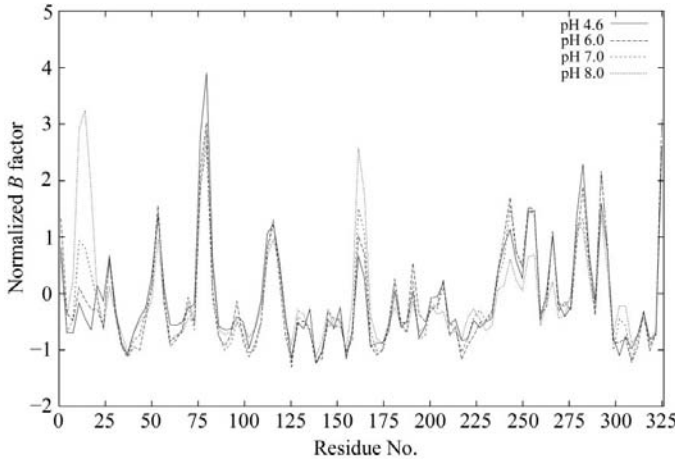

Figure 2
Normalized *B* factors of C^{α} atoms of rhizopuspepsin at different pH values.

As seen in Fig. 2, the *B* factors of the loop (Asn13 is at the tip of the loop) between the two N-terminal strands gradually increase as the pH increases and the change is quite pronounced at pH 8.0. Similarly, the *B* factors of loop 154–174 also show a considerable and gradual increase as a consequence of increase in the pH. These observations and the fact that these two loops are close to each other in the structure suggest that the pH-assisted denaturation of the enzyme probably originates from this region. The residue with the highest *B* factor, Asn13, could be considered as the hinge point, equivalent to Ala13 in cathepsin D, which is described as the pivot point about which the strand rotates and relocates itself and occupies the active site. Beyond pH 8.0, the N-terminal β-strand in rhizopuspepsin would probably relocate itself into the active site to achieve a stable conformation similar to that reported for the high-pH structure of cathepsin D. However, the possibilities of other adaptive mechanisms in order to retain the structure cannot be ruled out, as it is unlikely that the N-terminal segment of rhizopuspepsin will have a structure at high pH that is similar to that of the high-pH form of cathepsin D, since it has no positively charged residue corresponding to Lys8 of cathepsin D which blocks and neutralizes the charge of the active aspartates. The high *B* factors and high C^{α} deviations shown in the loop probably indicate a structural state of the proteinase in which the N-terminal segment is about to dissociate itself

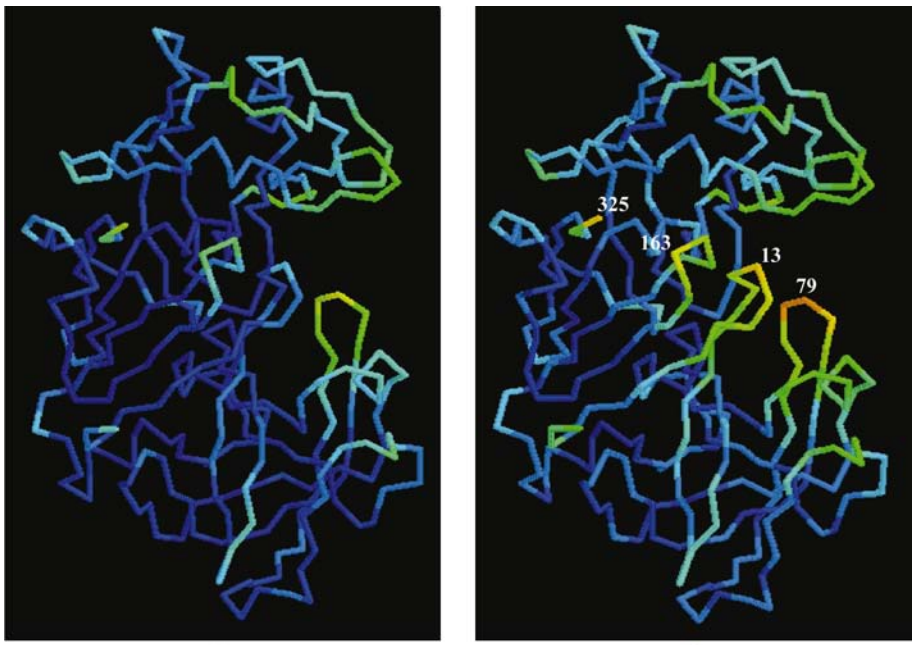

Figure 3
B-factor representation of rhizopuspepsin at (*a*) pH 6.0 and (*b*) pH 8.0. The figure was generated using the program *RASMOL* v.2.6. Temperature factors increase from blue to red.

from the protein, leading to either an unfolded form as in porcine pepsin (Tanaka & Yada, 2001) or another stable form of the protein as in cathepsin D (Lee *et al.*, 1998). However, it is clear that the structure is in a transition state at pH 8.0. The following section gives an account of the possible forces that enable such a conformational change.

3.2. A pH-sensitive region

In their effort to understand and explain the pH-dependent activity and stability of aspartic proteinases, Andreeva & Rumsh (2001) examined the role of uncharged polar residues in the vicinity of the active site, while Lin *et al.* (1993), based on solution studies of porcine pepsin, proposed that some of the acidic residues which are not located very close to the active site might cause alkaline denaturation of the enzyme. Since the active-site geometry of rhizopuspepsin remained unchanged over the pH range 4.6–8, we have focused our attention on regions containing polar residues which might bring about any structural changes with varying pH. The proteinase was visually searched for polar/charged residues within a sphere of 10.0 Å radius. Interestingly, we noticed only one such region and surprisingly it is very close to the regions which show high mobility at pH 8.0. Fig. 4 shows the region, with all residues within a sphere of 7.5 Å radius including all hydrogen bonds between the residues. Furthermore, to find whether this region being highly polar/charged is a characteristic feature of this family of enzymes, we compared the equivalent regions in the crystal structures of the active form of aspartic proteinases from ten other sources (PDB codes 3app, 4ape, 1mpp, 2asi, 1am5, 1psn, 4cms, 4pep, 1lya and 1bsf).

Table 4
Weakening of interactions involving charged residues in the pH-sensitive region as pH increases.

		Distance (Å)			
Protein atom 1	Protein atom 2	pH 4.5	pH 6.0	pH 7.0	pH 8.0
Lys305 NZ	Asp14 OD1	2.71	2.69	2.68	3.02
Glu325 OE2	Asn163 OD1	3.17	3.01	2.92	3.57
Lys160 NZ	Asp274 OD2	3.15	3.11	3.20	3.45
Glu325 OE1	Lys160 NZ	3.18	3.42	3.29	3.50

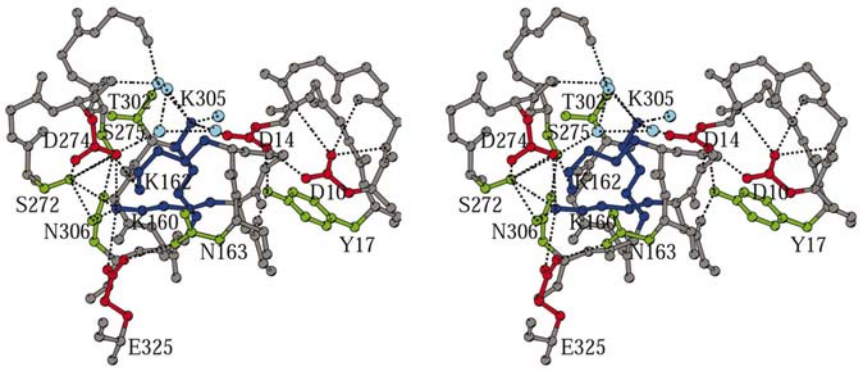

Figure 4
The pH-sensitive region in rhizopuspepsin. Figs. 4, 5 and 6 were generated using the program *MOLSCRIPT* (Kraulis, 1991).

In general, this region seems to be highly rich in charged amino acids, although the residues are not totally conserved. While Lys160, Lys162 and Glu325 are not conserved, Asp10 and Asp14 are partially conserved, Lys305 is mostly a lysine or an arginine and Asp274 is either an aspartate or a glutamate. The differences in this region found among the members of the aspartic proteinase family might explain the differences in pH optimum between different proteinases. At high pH, there could be a change in the charge distribution among the ionizable groups of the residues in this region, which in turn could trigger the movement of the first strand of the inter-domain β-sheet through the hinge point Asn13. This opens up scope for many mutational experiments, such as mutation of any of the charged residues in this region in order to probe the stability of the enzyme as a function of pH or to design enzymes that are more stable under conditions away from their pH optimum. Most of the hydrogen bonds in this region did not show much variation between the different forms. However, the hydrogen bonds Lys305 NZ$\cdots$Asp14 OD1, Glu325 OE2$\cdots$Asn163 OD1, Lys160 NZ$\cdots$Asp274 OD2 and Glu325 OE1$\cdots$Lys160 NZ, most of which are ionic interactions, became progressively weaker with the increase in pH from 4.6 to 8.0 (Table 4).

3.3. Hydrogen bonds in different pH forms

Hydrogen bonds between protein atoms were analysed in all four structures. There is no instance where a main chain-to-main chain hydrogen bond has undergone any noticeable change. Similarly, apart from the hydrogen bonds mentioned in the pH-sensitive region described above and a few changes involving the flap region, there are no other changes, even when side-chain hydrogen bonds are considered. This further confirms the existence of the pH-sensitive region which plays a role in pH-dependent conformational changes for regulation of catalysis.

3.4. Solvent structure

Hydrogen bonds involving all the waters were examined and compared between the four pH forms. Of these waters, the 17 conserved waters identified and discussed because of their functional and structural significance in the aspartic proteinase family (Prasad & Suguna, 2002) were analysed more critically. Hydrogen-bonding interactions involving these water molecules were almost conserved except for those with Wat510 and Wat513, as discussed below. Changes in solvent structure as the pH is varied are usually expected near imidazole groups, but interestingly rhizopuspepsin does not contain any histidine residues.

Recently, two articles (Prasad & Suguna, 2002; Andreeva & Rumsh, 2001) have discussed the functional role played by Wat510, in which it was observed that the hydrogen bond of this water with Tyr77 OH

becomes stronger in the complexes (2.79 Å in rhizopuspepsin) when compared with the native unbound form of the enzymes (3.03 Å). The same hydrogen bond becomes even weaker at pH 8.0 (3.36 Å) when compared with the pH 4.6, 6.0 and 7.0 forms (Fig. 5). It is observed that a strong hydrogen bond between Asp79 OD1, the residue at the tip of the flap, and Wat760 was broken (4.14 Å between these atoms) at high pH. Consequently, the flap seems to have become flexible and moved away from the active site, which is supported by the high C^{α} deviations in this region. This movement of the flap away from the active site further resulted in the displacement of Tyr77 OH away from Wat510, weakening the hydrogen bond. This seems to be another strategy by which the aspartic proteinase can regulate the efficiency of catalysis. The weaker the hydrogen bond between Tyr77 OH and Wat510, the lesser the catalytic efficiency.

The two domains of aspartic proteinases are related by an approximate twofold axis passing through Wat507. The two active aspartates are related by this dyad. Wat513 is shown to be another conserved water which is related to Wat502 by the same dyad (Prasad & Suguna, 2002). Similar to Wat502, Wat513 stabilizes the two ψ-loops by forming hydrogen bonds with Asp33 OD2 and Thr219 O. It also stabilizes the flexible loop between the two N-terminal β-strands by forming strong hydrogen bonds with the O and the N atoms of Tyr17 (Fig. 6). It also forms hydrogen bonds with two other waters, *viz*. Wat515 and Wat571. Interestingly, at pH 8.0 Wat513 moves away from the loop but continues to maintain strong hydrogen bonds with the ψ-loops on which the active aspartates are located and additionally forms two hydrogen bonds with Wat718 and a new water Wat876 at pH 8.0. Consequently, the strong hydrogen bonds of Wat513 with Tyr17 N and Tyr17 O are completely broken, thereby destabilizing the loop, which could also have contributed to the high *B* factors and deviations of this region.

The remaining invariant waters (approximately 200 in number) common to all pH forms were examined using graphics for any considerable deviations in the hydrogen-bonding distances. Approximately 10% of the waters showed gradual changes in the hydrogen bonds. We could identify a set of ten waters whose hydrogen bonds had become gradually weaker and another set of ten waters where the hydrogen bonds had become stronger. Unlike the 17 conserved waters, which are mostly localized in the N-terminal domain, these sets of waters do not seem to be localized in any domain or region in the proteinase. However, it is observed that most of them are either in the active-site cleft or on the surface. The hydrogen bonds involving Wat752, Wat760 and Wat571 are in the active-site region and have become much stronger at higher pH (pH 8.0) when compared with pH 4.6, 6.0 and 7.0. It is well known that the waters in the active site are displaced by the substrate. The implication of the above waters forming stronger hydrogen bonds is that a higher amount of energy will need to be expended by the substrate in displacing the waters under unfavourable pH conditions.

4. Conclusions

An attempt has been made to find the structural basis for the influence of pH on the function of rhizopuspepsin, one of the aspartic proteinases, by analysing its structure as a function of

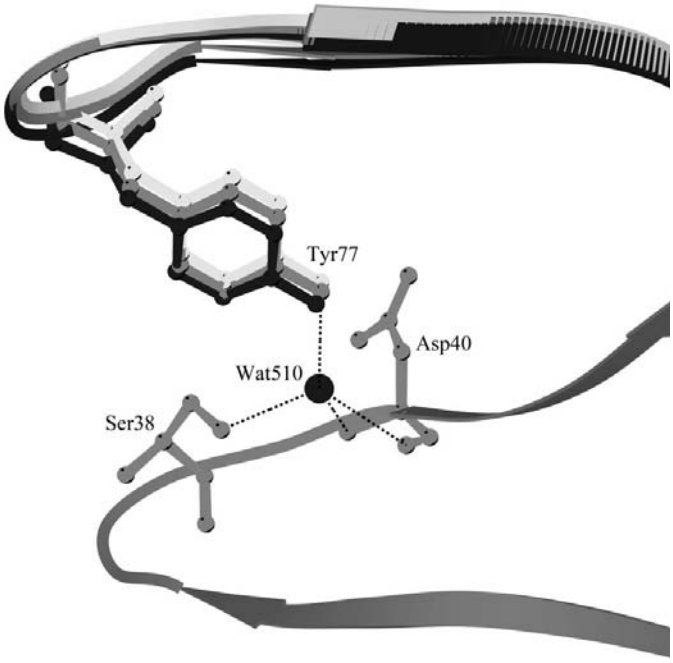

Figure 5
Weakening of the hydrogen bond between Wat510 and Tyr77 OH at pH 8.0. Tyr77 in the native structure (2apr) is shown in black, in the complex with a reduced inhibitor (3apr) in dark grey and in the pH 8.0 form in light grey.

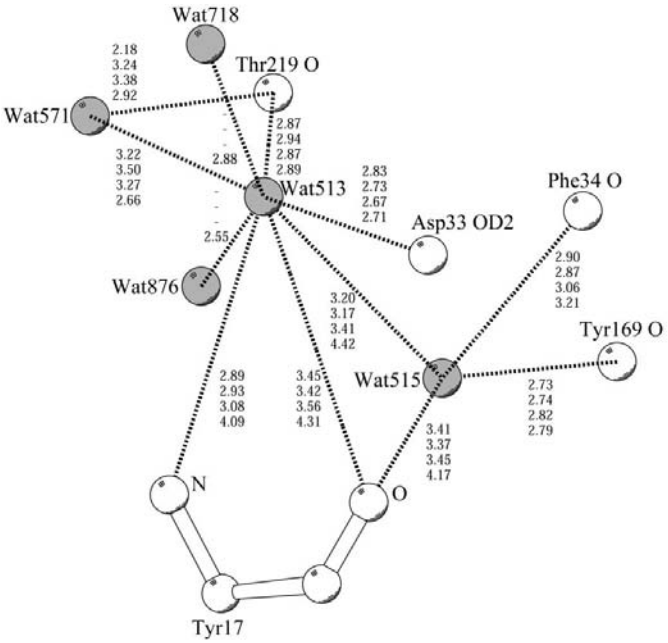

Figure 6
Breaking of the hydrogen-bonding network between Tyr17 of the peptide and the rest of the structure, destabilizing the N-terminal loop at high pH. The hydrogen-bonding distances are for the structures at pH 4.6, 6.0, 7.0 and 8.0 from top to bottom.

pH. The analysis revealed the beginning of unfolding of the structure at high pH, manifested by the high temperature factors of certain loops and the weakening of the interactions between these loops. We have identified one pH-sensitive region in the structures of 11 aspartic proteinases. This observation is expected to suggest a new set of protein-engineering experiments in this sensitive region to investigate further the opportunities to develop recombinant pH-resistant aspartic proteinases which have industrial applications. It is realised that the sensitivity of the protein to pH is a very complex phenomenon involving many subtle intra-protein interactions, including changes in the solvent–protein interactions. While the activity is turned on or off through large conformational changes, the efficiency may be influenced by changes in some important interactions in the enzyme.

We thank Dr D. R. Davies of the National Institutes of Health, USA for a generous gift of rhizopuspepsin. Intensity data were collected at the X-ray Facility for Structural Biology supported by the Department of Science and Technology (DST) and the Department of Biotechnology (DBT). Computations were carried out at the Bioinformatics Centre and Graphics Facility (both supported by DBT) and the Supercomputer Education and Research Centre at the Institute. The work is funded by the Council of Scientific and Industrial Research.

References

Andreeva, N. S. & Rumsh, D. (2001). *Protein Sci.* **10**, 2439–2450.
Berisio, R., Sica, F., Lamzin, V. S., Wilson, K. S., Zagari, A. & Mazzarella, L. (2002). *Acta Cryst.* D**58**, 441–450.
Bernstein, N. K. & James, M. N. G. (1999). *Curr. Opin. Struct. Biol.* **9**, 684–689.
Biswal, B. K., Sukumar, N. & Vijayan, M. (2000). *Acta Cryst.* D**56**, 1110–1119.
Brünger, A. T., Adams, P. D., Clore, G. M., DeLano, W. L., Gros, P., Grosse-Kunstleve, R. W., Jiang, J.-S., Kuszewski, J., Nilges, M., Pannu, N. S., Read, R. J., Rice, L. M., Simonson, T. & Warren, G. L. (1998). *Acta Cryst.* D**54**, 905–921.
Bullough, P. A., Hughson, F. M., Skehel, J. J. & Wiley, D. C. (1994). *Nature (London)*, **371**, 37–43.
Carr, C. M. & Kim, P. S. (1993). *Cell*, **73**, 823–832.
Coates, L., Erskine, P. T., Wood, S. P., Myles, D. A. & Cooper, J. B. (2001). *Biochemistry*, **40**, 13149–13157.
Cohen, G. H. (1997). *J. Appl. Cryst.* **30**, 1160–1161.
Davies, D. R. (1990). *Annu. Rev. Biophys. Biophys. Chem.* **19**, 189–215.
Dixon, M. M., Brennan, R. G. & Matthews, B. W. (1991). *Int. J. Biol. Macromol.* **13**, 89–96.
Gursky, O., Badger, J., Li, Y. & Caspar, D. L. (1992). *Biophys. J.* **63**, 1210–1220.
Guss, J. M., Harrowell, P. R., Murata, M., Norris, V. A. & Freeman, H. C. (1986). *J. Mol. Biol.* **192**, 361–387.
Hendrickson, W. A. & Konnert, J. H. (1981). *Biomolecular Structure, Conformation, Function and Evolution*, edited by R. Srinivasan, Vol. 1, pp. 43–57. Oxford: Pergamon Press.
Hofmann, T., Hodges, R. S. & James, M. N. G. (1984). *Biochemistry*, **23**, 635–643.
Jones, T. A., Zou, J. Y., Cowan, S. W. & Kjeldgaard, M. (1991). *Acta Cryst.* A**47**, 110–119.
Kraulis, P. J. (1991). *J. Appl. Cryst.* **24**, 946–950.
Kumaran, D., Eswaramoorthy, S., Furey, W., Sax, M. & Swaminathan, S. (2001). *Acta Cryst.* D**57**, 1270–1275.
Laskowski, R. A., MacArthur, M. W., Moss., D. S. & Thornton, J. M. (1993). *J. Appl. Cryst.* **26**, 283–291.
Lee, A. Y., Gulnik, S. V. & Erickson, J. W. (1998). *Nature Struct. Biol.* **5**, 866–871.
Lin, X.-I., Loy, J. A., Sussmann, F. & Tang, J. (1993). *Protein Sci.* **2**, 1383–1390.
Lubkowski, J., Dauter, Z., Yang, F., Alexandratos, J., Merkel, G., Skalka, A. M. & Wlodawer, A. (1999). *Biochemistry*, **38**, 13512–13522.
Mavridis, A., Tulinsky, A. & Liebman, M. N. (1974). *Biochemistry*, **13**, 3661–3666.
Nar, H., Messerschmidt, A., Huber, R., van de Kamp, M. & Canters G. W. (1991). *J. Mol. Biol.* **221**, 765–772.
Otwinowski, Z. & Minor, W. (1997). *Methods Enzymol.* **276**, 307–326.
Prasad, B. V. L. S. & Suguna, K. (2002). *Acta Cryst.* D**58**, 250–259.
Ramachandran, G. N., Ramakrishnan, C. & Sasisekharan, V. (1963). *J. Mol. Biol.* **7**, 95–99.
Sali, A., Veerapandian, B., Cooper, J. B., Moss, D. S., Hofmann, T. & Blundell, T. L. (1992). *Proteins Struct. Funct. Genet.* **12**, 158–170.
Suguna, K., Bott, R. E., Padlan, E. A., Subramanian, E., Sheriff, S., Cohen, G. H. & Davies, D. R. (1987). *J. Mol. Biol.* **196**, 877–900.
Tanaka, D. & Yada, R. Y. (2001). *Protein Eng.* **4**, 669–674.
Vendlen, R. L. & Tulinsky, A. (1973). *Biochemistry*, **12**, 4193–4200.
Yang, F. & Phillips, G. N. Jr (1996). *J. Mol. Biol.* **256**, 762–774.